A beetle antifreeze protein protects lactate dehydrogenase under freeze-thawing

Celeste Rodriguez[a], Seyed Sajjadi [b], Ravinder Abrol *[b], Xin Wen*[a]

[a] *Department of Chemistry and Biochemistry, California State University Los Angeles, Los Angeles, CA 90032, USA*

[b] *Department of Chemistry and Biochemistry, California State University Northridge, CA, 91330, USA*

E-mail address: xwen3@calstatela.edu (X. Wen); abrol@csun.edu (R. Abrol)

Keywords: freeze-thawing, freeze denaturation, freeze-labile protein stabilization, antifreeze protein

Abstract

Effects of a beetle antifreeze proteins (AFP) from *Dendroides canadensis* (DAFP-1) on a model freeze-labile enzyme, lactate dehydrogenase (LDH), were investigated under freezing and thawing conditions. The presence of DAFP-1 can effectively protect the enzymatic activity of LDH upon repeated freezing and thawing and the protective role of DAFP-1 is more significant than that of bovine serum albumin (BSA), a common protectant for freeze-labile proteins. The results of circular dichroism (CD) spectroscopy suggest that the presence of DAFP-1 provides protection to the denaturation of LDH under freezing and thawing. The molecular dynamics (MD) simulation of DAFP-1 and LDH suggests that DAFP-1 interacts with LDH using its ice-binding surface (IBS)

and mainly through its arginine residues. A mutant of DAFP-1, where all the arginine residues were replaced by alanine residues, lost its effect in protecting LDH under freezing and thawing. The results demonstrated that DAFP-1 is an effective protectant for a freeze-labile protein under freezing and thawing and the arginine residues in DAFP-1 are important for its protective role. By correlating the protective effect of an AFP with its structure, new insights in the identification and development of effective protectants for freeze-labile proteins were provided.

1. Introduction

Liquid water plays an important role in governing the structure and function of biological macromolecules [1]. Significant adverse consequences associated with the solidification of water can occur to not only living organisms (e.g., freeze injury, death), but also various processes of biological macromolecules [2]. For example, the productions of proteins and protein formulations are now an indispensable part of industry, where freezing is frequently applied to protein solutions in order to slow down undesirable chemical denaturation for extended period storage. However, stresses during the freezing and thawing process, such as cold temperature, large variations in pH, ice formation, freeze-concentration, and/or crystallization of solutes, can destabilize proteins and cause protein denaturation and aggregation [2-6]. Consequently, severe function loss often occurs to proteins under freezing and thawing, which has been a major concern for the long-term storage of freeze-labile proteins.

Lactate dehydrogenase (LDH) is a ubiquitous cytosolic enzyme for the interconversion of pyruvate and lactate driven by NADH/NAD+ in cells and its release into serum or culture media is one of

the most important biomarkers for tissue damage or cell death [7, 8]. However, LDH is sensitive to freezing and noticeably loses its activity after thawing, which limits its storage time [8]. Therefore, it is necessary to improve the freezing resistance of LDH. In fact, LDH has been utilized as a common model protein in the development of stable pharmaceutical formulations [9]. Experimental evidence has shown that LDH and some other proteins denature at the ice-water surface and ice formation is a critical destabilizing factor, among the others (e.g., cold temperature, freeze-concentration), for the function loss of these proteins upon freezing of the aqueous solutions [10, 11]. It has been reported that LDH loses its activity during freezing due to ice formation and its exposure to the ice-water interface [11-13].

In order to protect LDH and other proteins during the freezing and thawing process, additives are often used as co-solutes. Protective effects of additives, such as certain proteins, sugars, salts, and surfactants, on LDH and other labile proteins under freezing have been reported [4, 9, 14-20]. Despite the discovery of various protective molecules, each has its own advantages and disadvantages. For instance, low molecular weight sugars and salts, the most common types of protectants, are generally low cost and stable, but are less effective and prone to crystallization during freezing [4, 14, 16]. Comparing to the sugars and salts, proteins and non-ionic surfactants can be highly effective protectants, however, their available types are limited and they are more expensive and less studied [4, 9, 15, 18, 21, 22]. The identification and development of protectants is traditionally through trial and error, while many known effective protective agents can be found in organisms living in freezing habitats that have evolved in nature to enable physiological processes and survival in those freezing habitats.

Antifreeze proteins (AFPs) evolved in many cold-adapted organisms, such as fish, insect, and plant, are known to inhibit ice formation and growth and thus provide protection for these organisms from freeze damage in a noncolligative manner [23-25]. Through its functional surface or site, referred to as the ice-binding surface (IBS), an AFP can adsorb onto specific ice crystal surfaces and control the formation and growth of the ice while exposes its hydrophilic non-ice-binding surface (NIBS) to liquid water [26-29]. The NIBS of an AFP, which is relatively more hydrophobic, when exposed to water, can significantly depress ice nucleation temperature and delay the time of ice nucleation; the exposure of the IBS to water, however, greatly promotes ice nucleation [27]. Due to the great structural diversity of AFPs whose structures are known, the IBS and NIBS of AFPs are not often structurally apparent, however, those of some other AFPs like the AFP studied here are structurally distinct (Figure 1). Owing to their unique abilities in controlling ice formation and the facts that many effective protective agents are found in organisms under freezing conditions, AFPs have naturally been considered and studied as potential protective agents for preservation of biological materials and macromolecules [30-35]. However, mixed results on their effectiveness in protecting freeze-labile proteins were achieved in different studies [30, 33] and the role of different AFPs in protecting freeze-labile proteins remains elusive, thereby impeding the identification and development of effective protective agents from this natural resource [30, 33-35].

In this study, we first investigated and demonstrated the protective effect of a beetle AFP from *Dendroides canadensis* (DAFP-1) on a model freeze-labile enzyme, lactate dehydrogenase (LDH), under freezing and thawing conditions. DAFP-1 has distinct IBS and NIBS. The IBS of DAFP-1, located on a relatively flat β-sheet consisting of short β-strands formed by repetitive arrays of

threonine residues that (Fig. 1), is readily distinguishable from its NIBS, which is on the opposite side of the protein [36]. Recent studies have reported that DAFP-1 can interact with many other molecules for its other roles. For example, the IBS of DAFP-1 can interact with crystalline nucleosides and carbohydrates [36-39] to control their crystallization and the arginine residues in DAFP-1 can interact with anionic and polyhydroxy co-solutes to enhance the antifreeze ability [40]. Here, we also sought to understand the possible mechanistic role of DAFP-1 in protecting LDH through a combined experimental and molecular dynamics (MD) simulation approach.

2. Materials and methods

2.1. Materials

All chemicals were purchased from either Sigma-Aldrich (St. Louis, MO) or Fisher Scientific (Pittsburgh, PA) at ACS grade or better (unless described elsewhere) and were used as received. Rabbit muscle lactose dehydrogenase (LDH, L-2500) and bovine serum albumin (BSA, A-7906) were purchased from Sigma-Aldrich (St. Louis, MO). Milli-Q water produced from a Synergy water system was used for the preparation of all solutions.

2.2. Protein expression and purification

The expression and purification of the AFP, an isoform from *Dendroides canadensis*, and the mutant AFP, R9/25/30/54A, followed the previously published procedure [40-42]. The mutations (i.e., R9A, R25A, R30A, and R54A) in the AFP were generated through site-directed mutagenesis with the QuickChange kit (Agilent Technologies) using the wild-type plasmid as a template and the mutant plasmid was confirmed by sequencing [41]. Briefly, the AFPs were expressed as a

fusion protein in *Escherichia coli* Origami B cells. The cells were harvested by centrifugation at 4 °C. After the cells were disrupted, the crude protein was purified using immobilized metal ion affinity chromatography (IMAC) (Ni-NTA agarose, Qiagen). The tags of the AFP were cleaved off with enterokinase (New England Biolabs) and then the resulting protein was further purified by using IMAC and ion exchange chromatography. The purified wild-type AFP and R9/25/30/54A were characterized using sodium dodecyl sulfate–polyacrylamide gel electrophoresis (SDS-PAGE) gel electrophoresis, matrix-assisted laser desorption ionization time-of-flight (MALDI-TOF) mass spectrometer, circular dichroism spectrometry, and differential scanning calorimetry, respectively, as previously described [40-42]. The purity of the AFP and the mutant AFP was assessed to be greater than 95% by high-performance liquid chromatography (HPLC) (Supplemental Information).

2.3. Enzyme assays

All the LDH sample solutions were prepared from a LDH solution containing 1.0 mg/mL in 10 mM phosphate buffer, pH 7.0. To prepare 1.00 mL of a sample LDH solution for freeze-thaw experiments, 50 µL of 1.0 mg/mL LDH solution was mixed with each of the individual additives (i.e., the AFP, BSA) and/or water in varying amounts. The concentrations of the AFP were from 1.7 to 80 µg/mL. The concentration of BSA was 5.0 mg/mL. The final LDH concentration in all the sample LDH solutions was 50 µg/mL.

One mL sample enzyme solution was pipetted into a 1.6-mL microcentrifuge tube, then placed in a freezer at -20°C. After the sample was completely frozen for a certain period of time (e.g., 24

hours, a week), the sample was then completely thawed at room temperature for an hour. Thawed samples were then subjected immediately to enzyme activity assays for the remaining enzymatic activity. A complete freeze-thaw cycle of a sample was counted by freezing the sample at -20 ºC for at least 16 hours and then completely thawing the sample at room temperature for an hour. This freeze-thaw cycle was repeated until the LDH sample in the absence of additives completely lost its activity. The freeze-thaw experiments were performed in triplicate for each LDH sample.

Activity of the enzyme was assayed by monitoring the formation of β-nicotinamide adenine dinucleotide, reduced (NADH) in absorbance at 340 nm spectrophotometrically. The assay medium consisted of 100 mM CAPS buffer (N-cyclohexyl-3-aminopropanesulfonic acid, Calbiochem) pH 10.0, 1 mM β-nicotinamide adenine dinucleotide (NAD+), and 24 mM lactate. To initiate the reaction, 10 µl of sample containing 50 µg/ml LDH was added into 990 µL of assay medium that was pipetted into a cuvette. Specific activity (SA) of the sample was determined by using the rate of LDH reaction calculated from the slope of the linear portion as described in the following equation: $SA = [(\Delta A/\Delta t) / (6.22 \times l \times c)] \times df$, where ΔA is absorbance difference in Δt, Δt is the time duration in minutes, l is the pathlength of the cuvette, which is 1 cm, c is protein concentration in mg/ml, df is the dilution factor, which is 100, and 6.22 is the millimolar extinction coefficient of NADH at 340 nm in mM^{-1} cm^{-1} [43]. The LDH activity of untreated samples was set to 100% for comparison. All measurements were performed in triplicate at 25 ºC using a Beckman Coulter UV/VIS spectrophotometer and D800 Spectrophotometer software was used to assay fractions.

2.4. Statistical analysis

The data of enzyme assays was further analyzed using one-way analysis of variance (ANOVA) and paired *t*-tests in Microsoft Office Excel 2016. A *p*-value of less than 0.05 was considered to be statistically significant.

2.5. Circular dichroism (CD) spectroscopy

Potential conformational changes of the AFP and the LDH after freeze-thaw cycles were analyzed using circular dichroism (CD) spectroscopy. Protein samples, the AFP, LDH, and the mixture of the AFP and LDH, were subjected to a freeze-thaw cycle once per week for three weeks. All protein samples were dissolved in in 0.1 M sodium phosphate buffer, pH 7.0. For the protein mixture, the AFP (162 µg/mL) and LDH (98 µg/mL) were mixed in equal volume. The concentrations of the AFP and LDH were 81 µg/mL and 49 µg/mL, respectively, in all the samples. Samples were centrifuged at 10,000 × *g* for 10 min at 4 °C. CD spectra were collected for untreated protein samples (before any freeze-thaw treatments) and treated proteins on a Jasco 810 spectropolarimeter (JASCO Inc.) at ambient temperature using a quartz cuvette with a path length of 0.1 cm. The far-UV CD spectrum of each sample was collected from 270 nm to 195 nm over three accumulations as previously described [40].

2.6. Structural modeling

Structure of rabbit LDH: The structure of full length sequence of rabbit LDH monomer was built by using the Swiss-Model server [44] and based on the PDB structure 3H3F [45] as a template. The resulting monomer was then aligned to each of the 4 monomeric units in the 3H3F tetramer to generate the structure of full-length and tetrameric rabbit LDH bound to 4 NADH

molecules. The resulting structure was embedded in a water box and subjected to 50ns of molecular dynamics (MD) simulations using the Amber biomolecular simulation package, the Amber ff99SB force field for proteins [46], and GAFF force field for NADH to relax the LDH tetrameric structure in its native environment. This was carried out in multiple steps, where first the water is relaxed keeping the protein fixed, and then both protein and water are relaxed together. The multiple structure snapshots from the MD simulation were analyzed to select a snapshot that represented an average LDH structure closest to all the snapshots.

Structure of DAFP-1: The structure of full-length sequence of DAFP-1 was built by using the Swiss-Model server [44] and based on the PDB structure 1EZG of the beetle, *Tenebrio molitor* [26] as a template. This structure was also embedded in a water box and subjected to 50ns of MD simulations using the Amber package and protocol as described above for rabbit LDH. The MD trajectories was analyzed to select a snapshot that represented an average DAFP-1 structure closest to all the snapshots.

Structures of LDH:DAFP-1 complex: The protein-protein interactions in LDH:DAFP-1 complexes were modeled through the Cluspro program [47] by using the average structures of LDH and DAFP-1 proteins obtained above. Two docking modes were used for DAFP-1: one mode utilizing its IBS surface for docking to LDH, and the other mode utilizing its NIBS surface for docking to LDH. The IBS surface showed stronger affinity for LDH compared to the NIBS surface (range of -939 kcal/mol to -676 kcal/mol for the IBS surface binding versus range of -672 kcal/mol to -483 kcal/mol for the NIBS surface binding). The top 21 complexes based on "Balanced" energy scoring function of Cluspro for the IBS mode were analyzed visually. Eight of those complexes were used to create an oligomeric LDH:DAFP-1 complex based on lowest energy non-overlapping

arrangement of DAFP-1 around the LDH tetramer, that resulted in the L_4D_8 complex shown in Fig. 5 in the main text.

Relaxing of the LDH:DAFP-1 complex: The above obtained L_4D_8 complex containing 4 NADH molecules was inserted in a water box and subjected to 100ns of MD simulations using the same MD protocol as mentioned earlier for the individual proteins to relax the complex in its physiological environment and to test the stability of the LDH-bound DAFP-1 molecules. The complex snapshots were saved every 100ps and analyzed using VMD [48] for noncovalent interactions between LDH and DAFP-1. This analysis is presented in Table 1 below.

3. Results and discussion

3.1. Protective effect of DAFP-1 on LDH enzymatic activity

To elucidate the potential role of AFPs in protecting freeze-labile proteins upon freezing, we assessed the effect of DAFP-1 on the enzymatic activity of LDH under freezing and thawing treatments. LDH (50 μg/mL) was initially subjected to a freeze-thaw cycle treatment in the absence and presence of DAFP-1. The freeze-thaw cycle treatment was overnight unless specified otherwise. As shown in Fig. 2, LDH lost about 20% of its activity in the absence of DAFP-1 after a freeze-thaw treatment. In contrast, when LDH was frozen and thawed in the presence of DAFP-1 at a range of different concentrations, the activity of the enzyme was protected to different levels (Fig. 2). The protective effect of DAFP-1 is generally more significant at the higher concentrations until the activity of the freeze-thaw treated LDH reaches to that of the untreated LDH. In particular, the enzymatic activity of LDH after a freeze-thaw treatment was protected to a full extent in the presence of DAFP-1 at 25 μg/mL, that is, the molar ratio of DAFP-1 to LDH is 8:1, while further increasing the concentration of DAFP-1 or the molar ratio of DAFP-1 to LDH (e.g., DAFP-1 is at

80 µg/mL and the molar ratio of DAFP-1 to LDH is 26:1) does not enhance the activity of LDH (Fig. 2).

Then, LDH (50 µg/mL), alone and in the presence of DAFP-1 (25 µg/mL), was subjected to multiple freeze-thaw cycle treatments and the resulting enzymatic activity was assayed for each sample after every treatment. After four freeze-thaw cycle treatments, the activity of LDH alone reduced dramatically and only remained about 45% of its original activity. In contrast, the presence of DAFP-1 significantly protects the enzymatic activity of LDH and the enzyme remained about 90% of its original activity even after six freeze-thaw cycle treatments (Fig. 3). The protective effect of DAFP-1 on the enzymatic activity of freeze-thaw treated LDH is more significant than that of bovine serum albumin (BSA), a common protectant for freeze-labile proteins. The protective effect of BSA is generally considered as nonspecific ones of high protein concentrations [49]. The protection by BSA was achieved at a much higher concentration in comparing to DAFP-1. After six freeze-thaw cycle treatments, the enzymatic activity of LDH remained about 50% of its original activity in the presence of BSA at 5 mg/mL (Fig. 3), in comparing to 90% of its original activity remained in the presence of DAFP-1 at 25 µg/mL. Considering their molecular weights difference, DAFP-1 (MW = 9 kDa) and BSA (MW = 66 kDa), DAFP-1 is also more efficient than BSA in protection of the freeze-labile enzyme on a molar basis.

3.2. Protective effect of DAFP-1 against LDH denaturation after freeze-thaw treatments

To assess the effects of freezing and thawing and the protective effects of the AFP on LDH denaturation, circular dichroism (CD) spectra of LDH alone and LDH in the presence of DAFP-1 were collected in the far-ultraviolet (UV) region at room temperature before and after freeze-thaw

treatments, respectively. The concentrations of LDH and DAFP-1 for the CD experiments were 0.7 μM and 18 μM, respectively, in order to obtain better signal-to-noise ratio in the far-UV CD region (Figure 4). Moreover, the resulting molar ratio of LDH and DAFP-1 for the CD experiment is 1:25, which is the highest tested molar ratio for the enzymatic activity assays (Figure 1). Since there is no statistical difference between the results for the molar ratios of 1:8 and 1:25 (Figure 1), the protective effects by DAFP-1 under these two ratios could be assumed to be similar.

The far-UV CD spectrum of LDH without freeze-thaw treatments exhibits two typical troughs at about 208 nm and 222 nm (Fig. 4a, LDH), which are the characteristics of a predominant α-helical structure [45]. After four freeze-thaw cycle treatments in 3-weeks, the intensities of the characteristic peaks of the LDH in the far-UV region reduced to almost zero, suggesting that in the absence of protectants, LDH may almost completely denature and/or the protein itself (i.e., LDH) may be almost completely lost due to precipitation/adsorption during the freeze-thaw treatments (Fig. 4a, FT LDH).

The far-UV CD spectra of the AFP before and after the same freeze-thaw treatments were also collected. The far-UV CD spectra of the DAFP-1 sample without freeze-thaw treatments and the DAFP-1 sample after the same freeze-thaw cycle treatments are very much alike (Fig. 4b), which indicates that the AFP does not denature upon the freeze-thaw treatments.

To investigate the protective effect of the AFP on the denaturation of LDH under freezing and thawing, the far-UV CD spectra of the mixture of LDH and DAFP-1 under the above freeze-thaw treatments was collected and then analyzed by subtracting the CD signal of DAFP-1. The resulting

CD signal is then the CD signal of the AFP-protected LDH after the freeze-thaw treatments. In contrast to that of LDH alone after the freeze-thaw treatments, which was completely almost lost, the CD signal of the AFP-protected LDH mostly remains that of a native LDH in solution (Fig. 4c, FT LDH'). The CD results suggest that the presence of DAFP-1 can protect LDH denaturation under repeated freeze-thaw treatments, which were in accordance with the activity assay results.

Moreover, to validate the background subtraction by subtracting the CD signal of DAFP-1 from the CD signal of the mixture of LDH and DAFP-1, the CD signal of the mixture of the two proteins and the sum of the CD signals for each individual proteins at the specific concentration were collected and compared. As shown in Fig. 4d, the CD signal of the mixture of the two proteins is almost identical to the sum of the CD signals of each individual proteins, suggesting that LDH undergoes negligible conformational changes upon the presence of DAFP-1. Therefore, it is a valid background subtraction and any potential interactions between DAFP-1 and LDH would be weak [50].

3.3. Potential interactions between the IBS of DAFP-1 and LDH

To examine potential interactions between LDH and DAFP-1, an oligomeric complex of LDH and DAFP-1 was built using the protein-protein docking method called ClusPro [47] as described in the section of structural modeling. There are 8 DAFP-1 molecules and 1 LDH tetramer in the system (i.e., a molar ratio of 8:1) reflecting the optimal ratio of DAFP-1 to LDH determined in the enzymatic assays (Fig. 2). As the IBS and NIBS of DAFP-1 are located on the opposite sides of the protein (Fig. 1), either the IBS surface of DAFP-1 or the NIBS surface of DAFP-1 was used to dock to the LDH tetramer during the protein-protein docking process, which led to the

identification of multiple binding modes. The binding affinities of the IBS and NIBS modes of DAFP-1 binding to LDH were then calculated and compared. The results indicate that the IBS binding mode of DAFP-1 has stronger binding affinity for LDH (range of -939 kcal/mol to -676 kcal/mol) compared to the NIBS binding mode of DAFP-1 (range of -672 kcal/mol to -483 kcal/mol). Consequently, eight of the IBS surface-utilizing sterically non-overlapping lowest energy conformations of DAFP-1 bound to the LDH tetramer were used to create the LDH:DAFP-1 oligomeric complex [$LDH_4(DAFP\text{-}1)_8$ or L_4D_8]. The L_4D_8 complex was relaxed in aqueous environment using molecular dynamics (MD) simulations with the AMBER force field and simulation program [46]. Throughout the simulation, all 8 DAFP-1 molecules stayed bound tightly to the LDH protein, which validates the stability of DAFP-1 utilizing its IBS surface to interact with the LDH tetramer.

In this L_4D_8 complex, four DAFP-1 molecules are bound directly to the four LDH protomers in the tetramer (one DAFP-1 per LDH protomer). The remaining four DAFP-1 molecules interact with the dimer or trimer interfaces of the tetrameric LDH (Fig. 5). The dominant interactions between LDH and DAFP-1 are through salt-bridges and hydrogen bonds. The residues on the IBS of DAFP-1 dominate the interactions between the AFP with LDH, in particular Arg25, Arg30, and Arg54 along with Thr39, Thr65, and Thr74 (Table 1). The side chains of Arg25, Arg30, Arg54 on DAFP-1, for example, electrostatically interact with those of Glu103, Glu224, and Asp285 on LDH, respectively (see Table 1 for all the interactions and their relative stability during the MD simulation). The IBS residues of DAFP-1 are engaged in 16 salt bridge interactions and 20 hydrogen bond interactions with LDH residues. In addition, none of the 8 DAFP-1 molecules

occlude the NADPH catalytic site on LDH, proposing that DAFP-1 binding should not interfere with LDH's catalytic function.

Moreover, the structural modeling of the L_4D_8 complex suggests that the IBS of DAFP-1 faces to LDH, while the NIBS of DAFP-1 is exposed to water and the arginine residues in DAFP-1 play a role in such a molecular arrangement. Fig. 6 shows one such set of salt-bridge interactions between the Arg residues on DAFP-1 and the Glu and Asp residues on LDH. To demonstrate the potential roles of arginine residues of DAFP-1 in protecting LDH, we prepared the mutant of DAFP-1, R9/25/30/54A, where all the arginine residues were replaced by non-polar residues, alanine. The wild-type DAFP-1 and the R9/25/30/54A mutant were demonstrated to possess similar structures and ice-binding function in previous studies [40-42]. The effect of the mutant, R9/25/30/54A, on protecting the enzymatic activity of LDH was examined in this study following the same procedures as above. As shown in Fig. 7, comparing to that of the wild-type DAFP-1, the protective effect of the mutant R9/25/30/54A on LDH under freezing and thawing was reduced significantly. Based on the interactions between DAFP-1 and LDH shown in Table 1, by removing the four arginine residues in DAFP-1, the mutant R9/25/30/54A, would lose 10 out of 16 salt-bridge interactions and 4 out of 20 hydrogen bond interactions between the IBS of DAFP-1 and LDH, which significantly weaken the association between the IBS of DAFP-1 and LDH. The results suggest that the arginine residues in DAFP-1 dominate the association between the IBS of DAFP-1 and LDH and the loss of the arginine residues greatly diminishes the protective effect of DAFP-1 on LDH under freezing and thaw.

3.4. Possible roles of DAFP-1 in protecting LDH

The identified protective effect of DAFP-1 may depend on its interactions with the protected molecule (i.e., LDH) and water. For example, the binding of DAFP-1 to the LDH dimer interfaces (Figure 5) may improve the integrity of the tetrameric enzyme during the freezing-thawing process. Furthermore, the contact of LDH with ice or ice-water interface, a major destabilizing factor of LDH under freezing and thawing [11], can be reduced because of such interactions. Moreover, the arrangement of DAFP-1 by burying the ice-nucleation-promoting IBS towards LDH, while exposing the ice-nucleation-depressing NIBS to water, may shield LDH from ice more effectively and the long side chains of the arginine residues might act as molecular clamps recognizing and/or assisting such arrangement of DAFP-1.

Interactions with the protected protein and/or water-ice interfaces have been reported for some known nonionic surfactants, which can effectively protect certain proteins under freezing and thawing. For instance, Tween 20 may stabilizes recombinant human factor XIII, a homodimeric protein that aggregates at the ice-water interface, mainly through competing with soluble aggregates for the interfaces to inhibit subsequent transition to insoluble aggregates [21], whereas Tween 80 may stabilize LDH during freezing and thawing mainly through its weak interactions with LDH [9].

There are also examples about the protective effects of several plant-based late embryogenesis abundant (LEA) proteins on LDH during freezing and thawing in the literature recently [22, 51]. Most LEA proteins are intrinsically disordered proteins (IDPs) with high hydrophilicity, while LEA_2 proteins are more hydrophobic adopting a stable fold in solution. Interestingly, the protective effects of LEA proteins on LDH under freezing and thaw are not restricted to their

structures in solution, that is, both disordered and structured LEA proteins (e.g., certain LEA_4 proteins and LEA_2 proteins, respectively) can protect LDH during freezing and thawing, while their roles may be different. For example, a disordered LEA_4 protein may protect LDH by primarily competing with LDH aggregates for adsorption to the air/water interfaces during freezing and thawing [51], which can resemble to the role of certain non-ionic surfactants (e.g., Tween 20). However, how a structured LEA_2 protein works effectively remains elusive [22]. The findings in this study may also provide an explanation for the protective role of a LEA_2 protein irrespective of the detailed structures of the two proteins, that is, similarly to DAFP-1, a LEA_2 protein might bind to the LDH dimer interfaces and reduce the contact of LDH with ice, thereby stabilizing LDH during the freezing-thawing process.

4. Conclusion

In summary, the protective effect of an AFP with structurally distinct IBS and NIBS on a model freeze-labile enzyme has been investigated and potential interactions between the IBS of an AFP and another protein have been shown. Specifically, the presence of DAFP-1 can effectively protect the enzymatic activity of LDH upon repeated freeze-thaw treatments. The MD simulation results show that assisted by the side chains of the arginine residues on its IBS, DAFP-1 utilizes its IBS to interact with LDH, while exposes its opposite NIBS to water. The mutant study further demonstrated the importance of arginine residues in the AFP's protective role supporting the MD simulation observations. This study provides new insights in understanding the protective role of AFPs against protein denaturation during freezing and thawing. The findings may also help explain the protective role of other structured proteins that can effectively protect freeze-labile proteins. Such understanding will help identify and design highly effectively protectants in various fields,

such as biopreservation and biologics formulations. It needs mention that the addition of protein-based protectants will reduce the purity of biological samples. Depending on the applications, further isolation may be required. For example, size exclusion HPLC can be used to isolate the added AFPs from LDH after thawing.

Acknowledgments

The authors thank Prof. John Duman at University of Notre Dame for cDNA of DAFP-1. X.W. thanks the supports from the National Institutes of Health under award number GM086249 and from the National Science Foundation under Grant No. 1644917. Thanks to Mr. Mitch Voda, Ms. Sona Mnatsakanyan, and Mr. Eric Yeung, for their help on enzymatic assays. R.A. thanks Department of Chemistry and Biochemistry at CSUN for partial support of this project.

References

[1] P. Ball, Water as an Active Constituent in Cell Biology, Chem. Rev. 108 (2008) 74-108.

[2] F. Franks, Biophysics and Biochemistry at Low Temperatures, Cambridge University Press 1985.

[3] F. Franks, The Properties of Aqueous Solutions at Subzero Temperatures, in: F. Franks (Ed.), Water and Aqueous Solutions at Subzero Temperatures, Springer US, Boston, MA, 1982, pp. 215-338.

[4] L. Kreilgaard, S. Frokjaer, J.M. Flink, T.W. Randolph, J.F. Carpenter, Effects of Additives on the Stability of Recombinant Human Factor XIII during Freeze-Drying and Storage in the Dried Solid, Arch. Biochem. Biophys. 360 (1998) 121-134.

[5] G.B. Strambini, M. Gonnelli, Protein Stability in Ice, Biophys. J. 92 (2007) 2131-2138.

[6] B.S. Chang, B.S. Kendrick, J.F. Carpenter, Surface-induced denaturation of proteins during freezing and its inhibition by surfactants, J. Pharm. Sci. 85 (1996) 1325-30.

[7] N. Papadopoulos, Clinical applications of lactate dehydrogenase isoenzymes, Ann. Clin. Lab. Sci. 7 (1977) 506-510.

[8] J.W. Starnes, Effects of storage time and freezing on the activity of lactate dehydrogenase released from rat hearts, FASEB J. 20 (2006) A1153-A1153.

[9] A. Hillgren, H. Evertsson, M. Aldén, Interaction Between Lactate Dehydrogenase and Tween 80 in Aqueous Solution, Pharm. Res. 19 (2002) 504-510.

[10] G.B. Strambini, E. Gabellieri, Proteins in frozen solutions: evidence of ice-induced partial unfolding, Biophys. J. 70 (1996) 971-976.

[11] B.S. Bhatnagar, R.H. Bogner, M.J. Pikal, Protein Stability During Freezing: Separation of Stresses and Mechanisms of Protein Stabilization, Pharm. Dev. Technol. 12 (2007) 505-523.

[12] R.H.M. Hatley, F. Franks, S.F. Mathias, The stabilization of labile biochemicals by undercooling, Process Biochem. 22 (1987) 169-172.

[13] E. Cao, Y. Chen, Z. Cui, P.R. Foster, Effect of freezing and thawing rates on denaturation of proteins in aqueous solutions, Biotechnol. Bioeng. 82 (2003) 684-690.

[14] W. Wang, Instability, stabilization, and formulation of liquid protein pharmaceuticals, Int. J. Pharm. 185 (1999) 129-188.

[15] T. Shimizu, T. Korehisa, H. Imanaka, N. Ishida, K. Imamura, Characteristics of proteinaceous additives in stabilizing enzymes during freeze-thawing and -drying, Biosci., Biotechnol., Biochem. 81 (2017) 687-697.

[16] W. Wang, Advanced protein formulations, Protein Sci. 24 (2015) 1031-1039.

[17] S.N. Timasheff, Solvent effects on protein stability: Current Opinion in Structural Biology 1992, 2:35…-39, Curr. Opin. Struct. Biol. 2 (1992) 35-39.

[18] K. Imamura, K. Murai, T. Korehisa, N. Shimizu, R. Yamahira, T. Matsuura, H. Tada, H. Imanaka, N. Ishida, K. Nakanishi, Characteristics of sugar surfactants in stabilizing proteins during freeze-thawing and freeze-drying, J. Pharm. Sci. 103 (2014) 1628-1637.

[19] J.F. Carpenter, J.H. Crowe, The mechanism of cryoprotection of proteins by solutes, Cryobiology 25 (1988) 244-255.

[20] K.-i. Izutsu, S. Yoshioka, T. Terao, Stabilizing effect of amphiphilic excipients on the freeze-thawing and freeze-drying of lactate dehydrogenase, Biotechnol. Bioeng. 43 (1994) 1102-1107.

[21] L. Krielgaard, L.S. Jones, T.W. Randolph, S. Frokjaer, J.M. Flink, M.C. Manning, J.F. Carpenter, Effect of tween 20 on freeze-thawing- and agitation-induced aggregation of recombinant human factor XIII, J. Pharm. Sci. 87 (1998) 1593-1603.

[22] N.X. Dang, A.V. Popova, M. Hundertmark, D.K. Hincha, Functional characterization of selected LEA proteins from Arabidopsis thaliana in yeast and in vitro, Planta 240 (2014) 325-336.

[23] A.L. DeVries, Glycoproteins as Biological Antifreeze Agents in Antarctic Fishes, Science 172 (1971) 1152-1155.

[24] Y. Yeh, R.E. Feeney, Antifreeze Proteins: Structures and Mechanisms of Function, Chem. Rev. 96 (1996) 601-618.

[25] J.A. Raymond, A.L. DeVries, Adsorption Inhibition as a Mechanism of Freezing Resistance in Polar Fishes, Proc. Natl. Acad. Sci. U.S.A. 74 (1977) 2589-2593.

[26] Y.-C. Liou, A. Tocilj, P.L. Davies, Z. Jia, Mimicry of ice structure by surface hydroxyls and water of a b-helix antifreeze protein., Nature 406 (2000) 322-324.

[27] K. Liu, C. Wang, J. Ma, G. Shi, X. Yao, H. Fang, Y. Song, J. Wang, Janus effect of antifreeze proteins on ice nucleation, Proc. Natl. Acad. Sci. U.S.A. 113 (2016) 14739-14744.

[28] D.J. Bowles, P.J. Lillford, D.A. Rees, I.A. Shanks, P.L. Davies, J. Baardsnes, M.J. Kuiper, V.K. Walker, Structure and function of antifreeze proteins, Philos. Trans. R. Soc. Lond. B Biol. Sci. 357 (2002) 927-935.

[29] P.L. Davies, Ice-binding proteins: a remarkable diversity of structures for stopping and starting ice growth, Trends Biochem. Sci. 39 (2015) 548-555.

[30] M. Griffith, C. Lumb, S.B. Wiseman, M. Wisniewski, R.W. Johnson, A.G. Marangoni, Antifreeze Proteins Modify the Freezing Process In Planta, Plant Physiol. 138 (2005) 330-340.

[31] D.O. Halwani, K.G.M. Brockbank, J.G. Duman, L.H. Campbell, Recombinant Dendroides canadensis antifreeze proteins as potential ingredients in cryopreservation solutions, Cryobiology 68 (2014) 411-418.

[32] I. Kratochvílová, M. Golan, K. Pomeisl, J. Richter, S. Sedláková, J. Šebera, J. Mičová, M. Falk, I. Falková, D. Řeha, K.W. Elliott, K. Varga, S.E. Follett, D. Šimek, Theoretical and experimental study of the antifreeze protein AFP752, trehalose and dimethyl sulfoxide cryoprotection mechanism: correlation with cryopreserved cell viability, RSC Advances 7 (2017) 352-360.

[33] M. Mangiagalli, M. Bar-Dolev, P. Tedesco, A. Natalello, A. Kaleda, S. Brocca, D. de Pascale, S. Pucciarelli, C. Miceli, I. Braslavsky, M. Lotti, Cryo-protective effect of an ice-binding protein derived from Antarctic bacteria, FEBS J. 284 (2017) 163-177.

[34] I.K. Voets, From ice-binding proteins to bio-inspired antifreeze materials, Soft Matter 13 (2017) 4808-4823.

[35] L. Weng, S.L. Stott, M. Toner, Exploring Dynamics and Structure of Biomolecules, Cryoprotectants, and Water Using Molecular Dynamics Simulations: Implications for Biostabilization and Biopreservation, Annu. Rev. Biomed. Eng. 21 (2019) null.

[36] X. Wen, S. Wang, J.G. Duman, J.F. Arifin, V. Juwita, W.A. Goddard, A. Rios, F. Liu, S.-K. Kim, R. Abrol, A.L. DeVries, L.M. Henling, Antifreeze proteins govern the precipitation of trehalose in a freezing-avoiding insect at low temperature, Proc. Natl. Acad. Sci. U.S.A. 113 (2016) 6683-6688.

[37] S. Wang, X. Wen, P. Nikolovski, V. Juwita, J. Fnu Arifin, Expanding the molecular recognition repertoire of antifreeze polypeptides: effects on nucleoside crystal growth, Chem. Commun. 94 (2012) 11555-11557.

[38] S. Wang, X. Wen, J.A. Golen, J.F. Arifin, A.L. Rheingold, Antifreeze Protein-Induced Selective Crystallization of a New Thermodynamically and Kinetically Less Preferred Molecular Crystal, Chem. Eur. J. 19 (2013) 16104-16112.

[39] S. Wang, X. Wen, A.L. DeVries, Y. Bagdagulyan, A. Morita, J.A. Golen, J.G. Duman, A.L. Rheingold, Molecular Recognition of Methyl a-D-Mannopyranoside by Antifreeze (Glyco)Proteins, J. Am. Chem. Soc. 136 (2014) 8973-8991.

[40] S. Wang, N. Amornwittawat, V. Juwita, Y. Kao, J.G. Duman, T.A. Pascal, W.A. Goddard, X. Wen, Arginine, a Key Residue for the Enhancing Ability of an Antifreeze Protein of the Beetle Dendroides canadensis, Biochemistry 48 (2009) 9696-9703.

[41] D. Brown, Role of arginine residues in the enhancing function of an antifreeze protein from the beetle Dendroides canadensis, MAI, Los Angeles, CA, 2012.

[42] X. Wen, S. Wang, J. Fielder, D. Brown, C. de La Fuente, V. Juwita, E.A. Houghton, M.A. Sacco, Enhancer Interactions with Antifreeze Protein: Mechanistic Insights into the Effect of Antifreeze Activity Enhancement, Biophys. J. 102 (2012) 461a.

[43] B.L. Horecker, A. Kornberg, THE EXTINCTION COEFFICIENTS OF THE REDUCED BAND OF PYRIDINE NUCLEOTIDES, J. Biol. Chem. 175 (1948) 385-390.

[44] A. Waterhouse, M. Bertoni, S. Bienert, G. Studer, G. Tauriello, R. Gumienny, F.T. Heer, T.A P. de Beer, C. Rempfer, L. Bordoli, R. Lepore, T. Schwede, SWISS-MODEL: homology modelling of protein structures and complexes, Nucleic Acids Res. 46 (2018) W296-W303.

[45] K. Świderek, A. Panczakiewicz, A. Bujacz, G. Bujacz, P. Paneth, Modeling of Isotope Effects on Binding Oxamate to Lactic Dehydrogenase, J. Phys. Chem. B 113 (2009) 12782-12789.

[46] D.A. Case, T.E. Cheatham III, T. Darden, H. Gohlke, R. Luo, K.M. Merz Jr., A. Onufriev, C. Simmerling, B. Wang, R.J. Woods, The Amber biomolecular simulation programs, J. Comput. Chem. 26 (2005) 1668-1688.

[47] D. Kozakov, D.R. Hall, B. Xia, K.A. Porter, D. Padhorny, C. Yueh, D. Beglov, S. Vajda, The ClusPro web server for protein–protein docking, Nat. Protoc. 12 (2017) 255.

[48] W. Humphrey, A. Dalke, K. Schulten, VMD: Visual molecular dynamics, J. Mol. Graphics 14 (1996) 33-38.

[49] Luciano A. Abriata, E. Spiga, Matteo D. Peraro, Molecular Effects of Concentrated Solutes on Protein Hydration, Dynamics, and Electrostatics, Biophys. J. 111 (2016) 743-755.

[50] S.M. Kelly, N.C. Price, Circular Dichroism to Study Protein Interactions, Curr. Protoc. Protein Sci. 46 (2006) 20.10.1-20.10.18.

[51] S. Koubaa, A. Bremer, D.K. Hincha, F. Brini, Structural properties and enzyme stabilization function of the intrinsically disordered LEA_4 protein TdLEA3 from wheat, Sci. Rep. 9 (2019) 3720.

Figures and Table

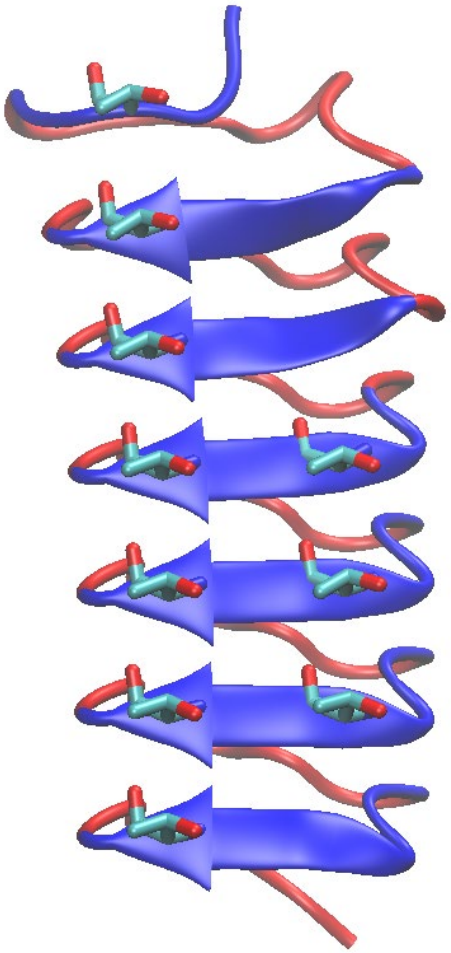

Fig. 1. The DAFP-1 model structure shown with its Ice-Binding Surface (IBS) in blue and Non-Ice-Binding Surface (NIBS) in red. The regularly spaced Threonine residues are shown as sticks.

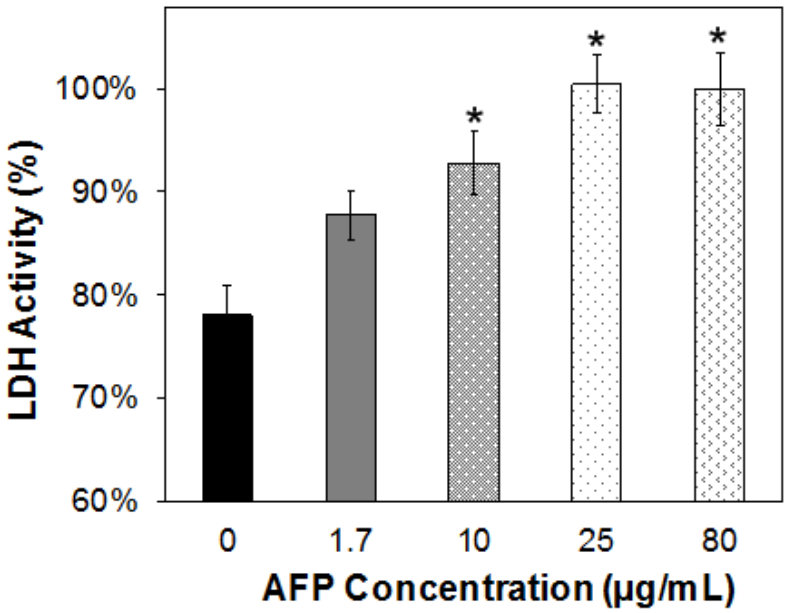

Fig. 2. Lactate dehydrogenase (LDH) activity in the absence and presence of a variety of AFP concentrations after a single freeze-thaw cycle. The concentration of LDH was 50 µg/mL. Values are shown as mean ± standard deviation. Asterisks indicate a significant difference at the level of $p < 0.05$ compared to the samples of LDH alone.

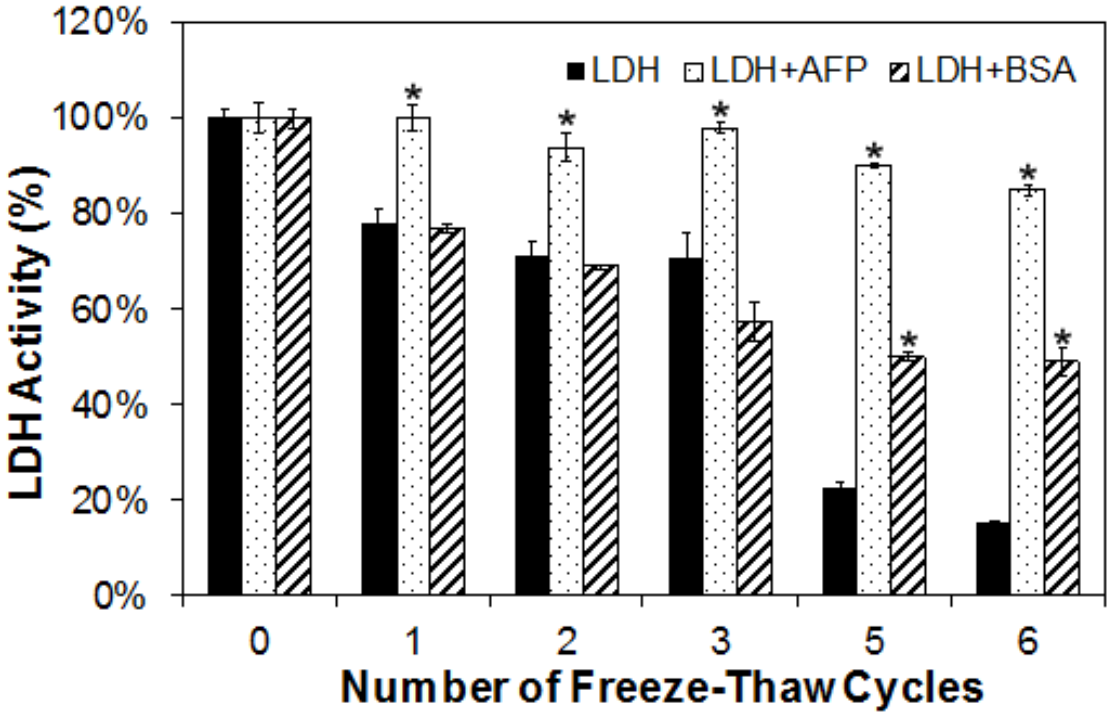

Fig. 3. Comparison of the cryoprotective effects of bovine serum albumin (BSA) and antifreeze protein (AFP) on lactate dehydrogenase (LDH) activity after a number of repeated freeze-thaw cycles over six days. The activities of LDH alone, LDH in the presence of AFP, and LDH in the presence of BSA are shown as black bars, dotted bars, and striped bars, respectively. The concentration of LDH was 50 μg/mL and the concentrations of BSA and the AFP were 5 mg/mL and 25 μg/mL, respectively. Values are shown as mean ± standard deviation. Asterisks indicate a significant difference at the level of $p < 0.05$ compared to the samples of LDH alone.

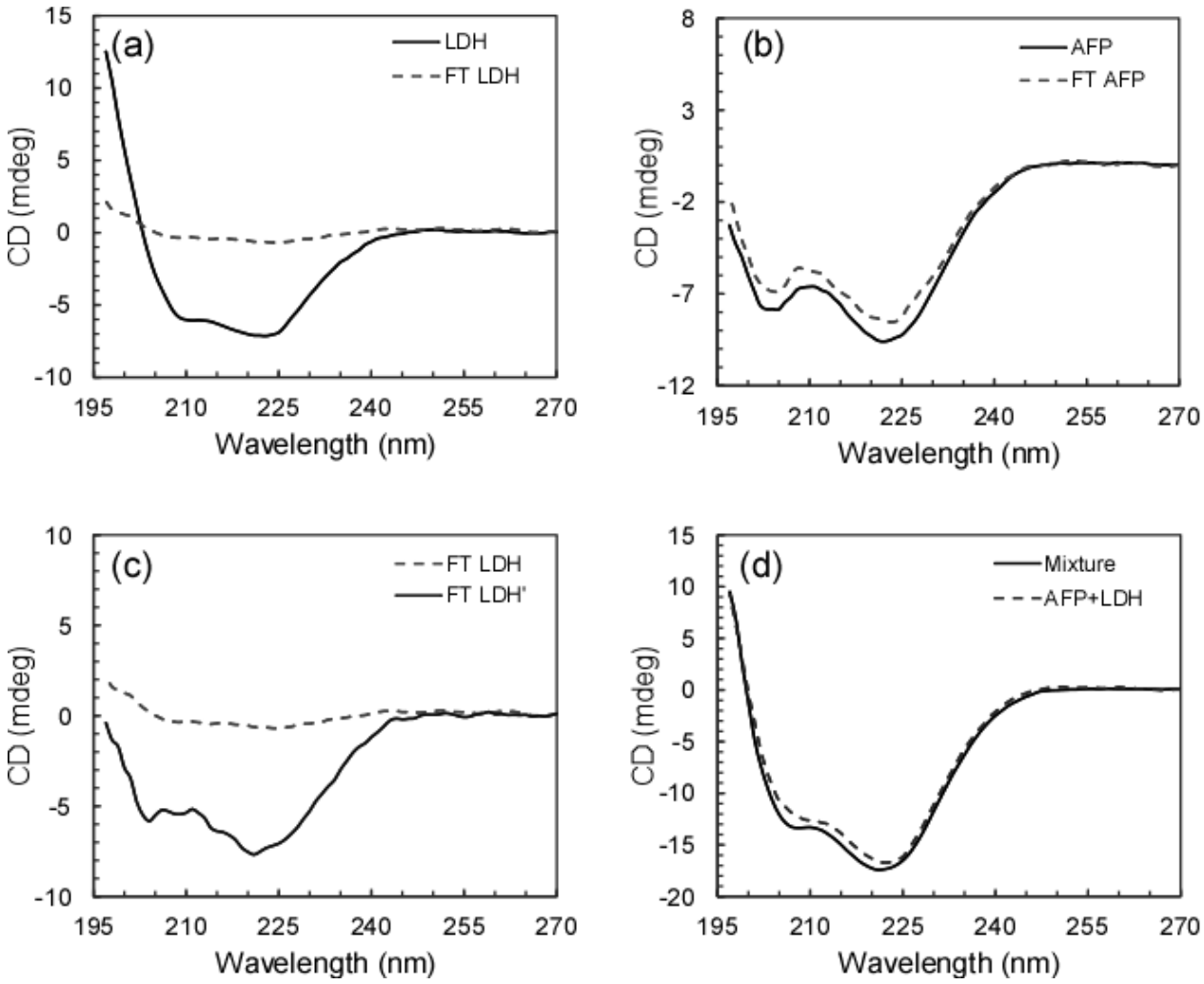

Fig. 4. Circular dichroism (CD) spectra of (a) LDH without any freeze-thaw treatments (LDH, solid line) and after four unprotected freeze-thaw treatments (FT LDH, dashed line; (b) DAFP-1 without any freeze-thaw treatments (AFP, solid line) and after four freeze-thaw treatments (FT AFP, dashed line); (c) four freeze-thaw treatments protected by DAFP-1 (FT LDH', solid line) where the CD signal of DAFP-1 was subtracted from the CD signal of the mixture of LDH and DAFP-1; and (d) the mixture of DAFP-1 and LDH (Mixture, solid line) and the sum of the CD spectra of LDH and DAFP-1 (AFP+LDH, dashed line). The LDH and DAFP-1 concentrations were 0.7 μM and 18 μM, respectively.

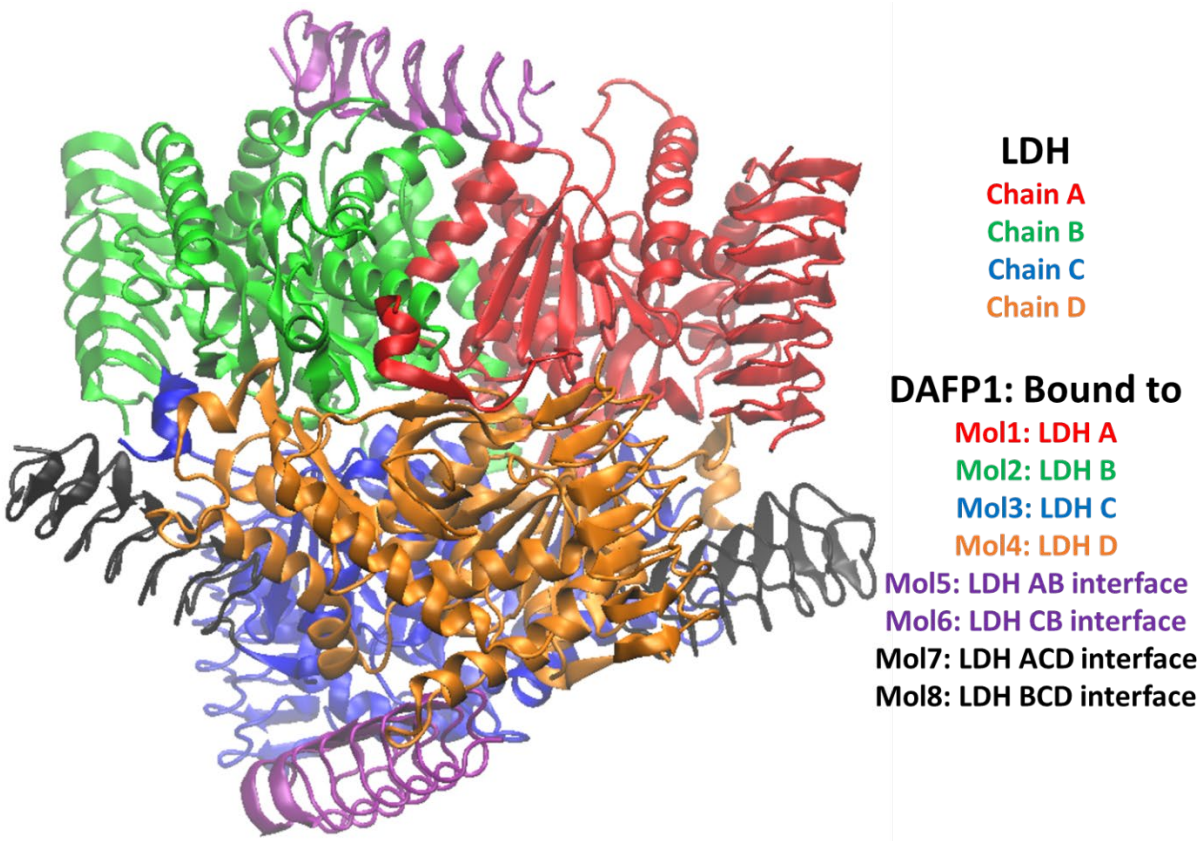

Fig. 5. A model of DAFP-LDH interactions. LDH Chain A (LDH A) is in red, LDH Chain B (LDH B) is in green, LDH Chain C (LDH C) is in blue, and LDH Chain D (LDH D) is in orange. The DAFP-1 molecule bound to LDH A is in red, the DAFP-1 molecule bound to LDH B is in green, the DAFP-1 molecule bound to LDH C is in blue, and the DAFP-1 molecule bound to LDH D is in orange. The DAFP-1 molecules bound to LDH AB and LDH CB interfaces are in Purple and the DAFP-1 molecules bound to LDH ACD and LDH BCD interfaces are in purple.

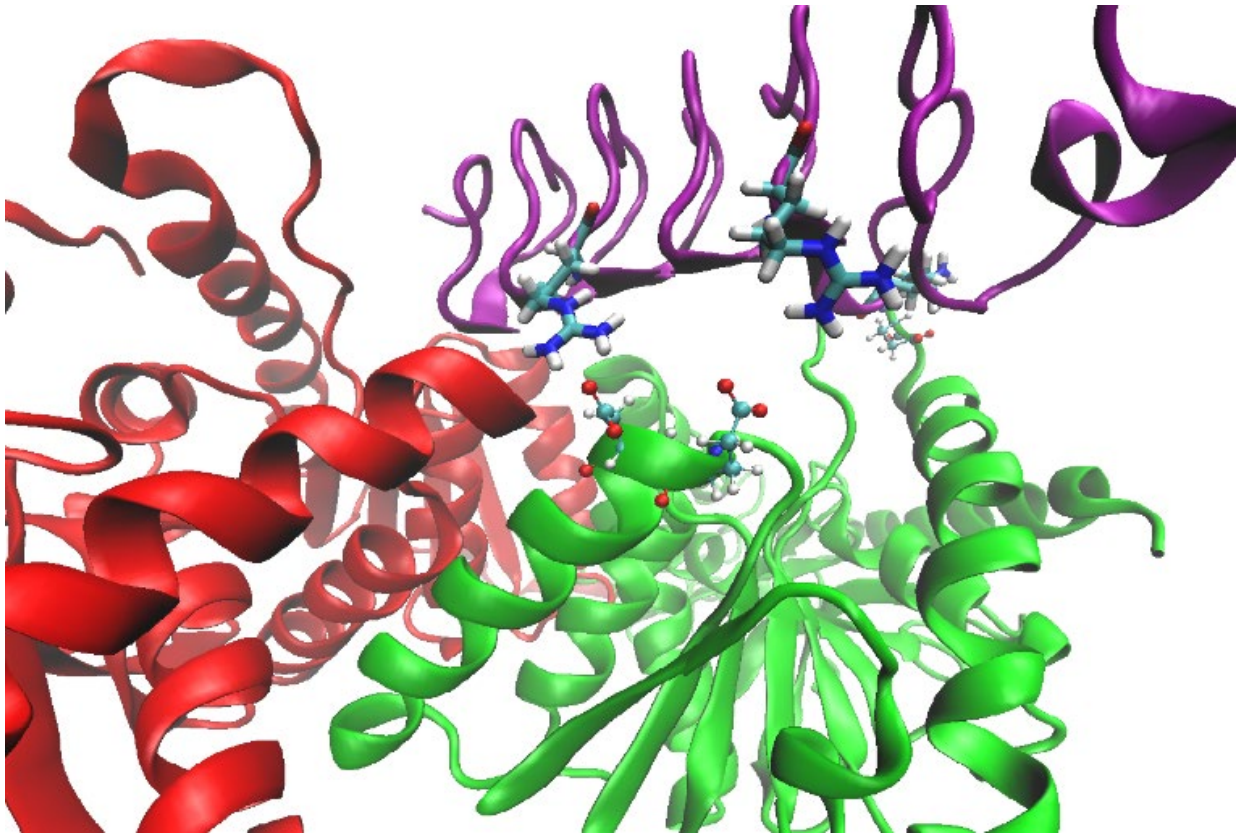

Fig. 6. A close-up view of two DAFP-1 Arginine residues (shown as sticks) sticking out of the DAFP-1 (purple) is shown interacting with the Glu/Asp residues (shown as balls-and-sticks) of LDH protomers (red and green) through salt-bridge interactions.

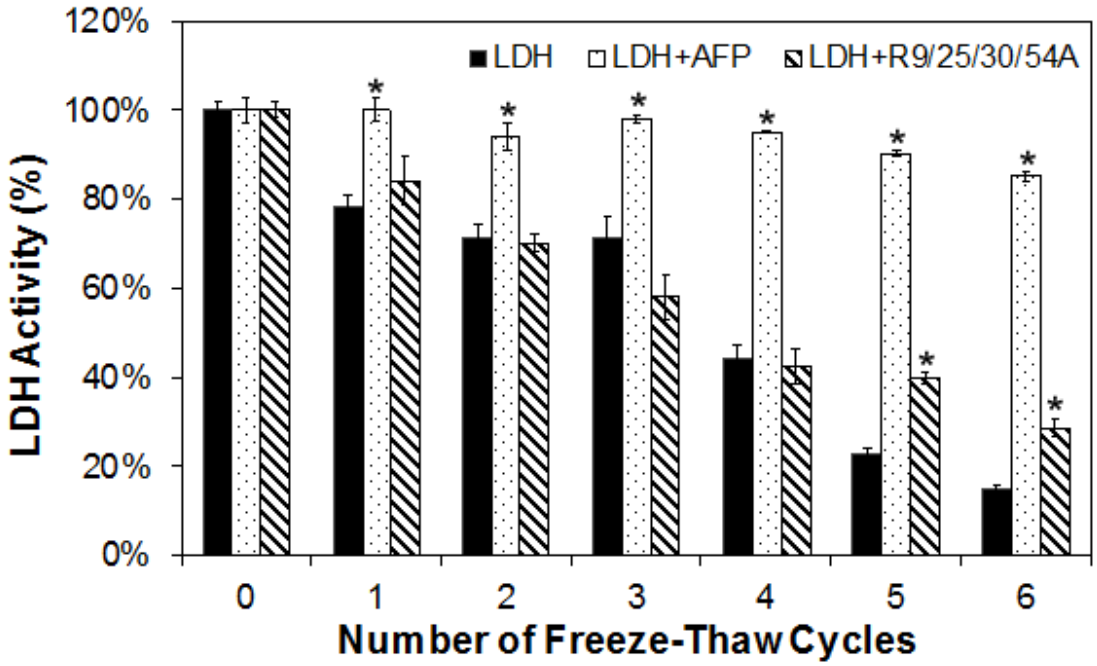

Fig. 7. Protective effects of the wild-type antifreeze protein (AFP) and the mutant AFP (R9/25/30/54A) on lactate dehydrogenase (LDH) activity after a number of repeated freeze-thaw cycles over six days. The activities of LDH alone (black bars) and LDH in the presence of AFP (dotted bars) were plotted for comparison. The activities of LDH in the presence of R9/25/30/54A are shown as striped bars. The concentration of LDH was 50 μg/mL and the concentrations of the AFP and the mutant were both 25 μg/mL. Values are shown as mean ± standard deviation. Asterisks indicate a significant difference at the level of $p < 0.05$ compared to the samples of LDH alone.

Table 1. Interacting residues between DAFP-1 and LDH. Interacting residues in DAFP-1 are shown in blue cells. Salt bridge interactions are shown in orange cells.

DAFP1 SITES	Donor	SC/BB[2]	Acceptor[1]	SC/BB[2]	Stability[3]
Ice Binding Surface Arginine Threonine Residues	S-ARG30	SideChain	D-GLU224	SideChain	93.5%
	D-SER78	BackBone	T-THR74	BackBone	89.2%
	R-ARG30	SideChain	B-PHE331	SideChain	84.2%
	P-ARG54	SideChain	A-ASP285	SideChain	83.3%
	B-LYS154	BackBone	R-THR65	SideChain	79.6%
	R-THR39	SideChain	B-SER150	BackBone	77.9%
	R-ARG54	SideChain	B-ASP285	SideChain	74.8%
	C-SER78	BackBone	S-THR74	BackBone	73.3%
	M-ARG54	SideChain	C-ASP55	SideChain	71.5%
	P-ARG30	SideChain	A-PHE331	SideChain	67.9%
	L-ARG25	SideChain	B-GLU103	SideChain	63.6%
	N-ARG54	SideChain	D-ASP285	SideChain	58.2%
	P-THR39	SideChain	A-SER150	BackBone	55.7%
	R-THR53	SideChain	B-GLY151	BackBone	52.1%
	L-ARG54	SideChain	B-ASP55	SideChain	38.4%
	P-THR41	SideChain	A-LYS148	BackBone	37.8%
	N-ARG30	SideChain	D-PHE331	SideChain	36.0%
	T-ARG30	SideChain	C-GLU224	SideChain	35.8%
	S-THR51	SideChain	D-GLU175	SideChain	32.5%
	N-THR74	SideChain	A-GLU15	SideChain	29.4%
	C-ASN122	SideChain	Q-THR26	SideChain	28.5%
	M-ARG54	SideChain	D-LYS242	BackBone	26.2%
	L-ARG30	SideChain	B-GLU54	SideChain	26.0%
	S-ARG54	SideChain	D-GLN225	SideChain	25.5%
Ice Binding Surface Other Residues	A-LYS13	BackBone	N-CYS76	BackBone	81.2%
	C-GLN232	SideChain	T-ASP78	SideChain	66.4%
	B-ARG98	SideChain	L-GLU50	SideChain	65.4%
	S-SER14	SideChain	C-ASP5	SideChain	60.2%
	D-GLN65	SideChain	T-ALA75	BackBone	58.7%
	C-GLN100	SideChain	M-GLU50	SideChain	45.5%
	N-CYS76	BackBone	A-LYS13	BackBone	44.9%
	A-ARG98	SideChain	L-ASP78	SideChain	40.2%
	B-HIE129	SideChain	R-GLU50	SideChain	33.1%
	A-LYS148	SideChain	P-ASP42	SideChain	30.0%
	A-HIE129	SideChain	P-GLU50	SideChain	29.1%
	B-LYS154	SideChain	R-ASP78	SideChain	27.2%
Non-Ice Binding Surface	D-LYS80	BackBone	T-PRO83	SideChain	59.5%
	D-ARG98	SideChain	M-PRO83	SideChain	58.7%
	D-LYS80	SideChain	T-PRO83	SideChain	53.5%
	D-ARG111	SideChain	M-PRO83	SideChain	37.0%
	C-ASP81	BackBone	S-PRO83	SideChain	30.6%
	D-GLU101	BackBone	M-SER79	BackBone	28.2%

[1]Chain-Residue, where chain A,B,C,D are for 4 LDH protomers and L,M,N,P,Q,R,S,T chains are for 8 DAFP1 molecules.

[2]SideChain or BackBone, representing the part of the residue involved in noncovalent interaction.

[3]Stability of the noncovalent interaction as a fraction of the time it is stable during the MD simulation. The interactions stable at least 25% of the time are generally considered significant and are shown in this table. The orange stability cells refer to salt-bridge interactions.

Supporting Information

A beetle antifreeze protein protects lactate dehydrogenase under freeze-thawing

Celeste Rodriguez[a], Seyed Sajjadi [b], Ravinder Abrol *[b], Xin Wen*[a]

[a] *Department of Chemistry and Biochemistry, California State University Los Angeles, Los Angeles, CA 90032, USA*

[b] *Department of Chemistry and Biochemistry, California State University Northridge, CA, 91330, USA*

E-mail address: xwen3@calstatela.edu (X. Wen); abrol@csun.edu (R. Abrol)

Table of Contents

1. HPLC analysis

The purity of DAFP-1 and the mutant R9/25/30/54A were assessed by HPLC. The HPLC analysis were performed on a Waters HPLC system consisting of a Waters 1525 binary HPLC pump, a Xbridge BEH200, 3.5 µm SEC HPLC column, 7.8 × 150 mm (Waters, Milford, MA) and a Waters 2998 photodiode array detector. The SEC buffer contained 0.10 M Na_2SO_4, 0.10 M sodium phosphate butter (pH 7.00), and 0.02% NaN_3. All the buffers and samples were filtered through a 0.1 µm filter and vacuum degassed before use. The flow rate was 1.0 mL/min at ambient temperature. The injection volume was 5 µl and the sample concentration was 0.3 mM. Elution was performed at a flow rate of 1.0 ml/min at ambient temperature. The eluates were monitored at 280 nm. Pure DAFP-1 and the mutant R9/25/30/54A were eluted at 5.00 and 4.96 minutes, respectively (Figure S1).

2. Supporting figures

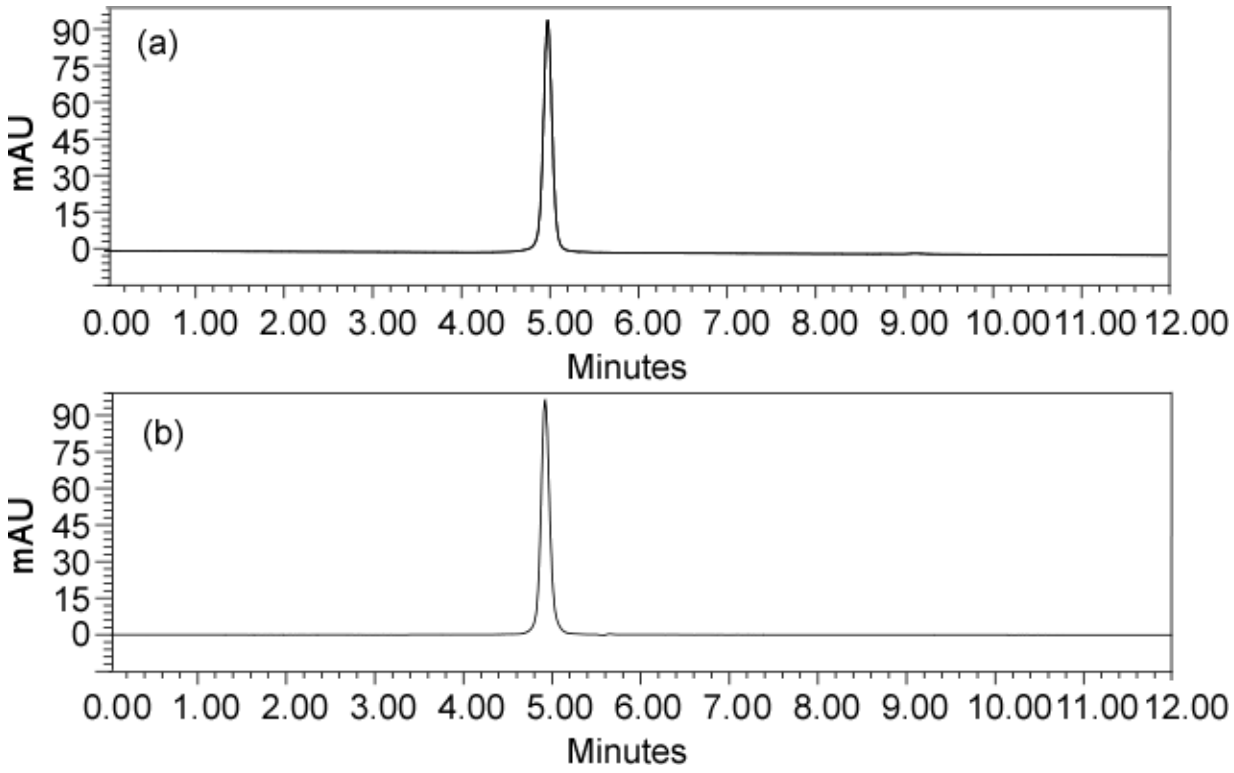

Figure S1. The HPLC chromatograms of (a) DAFP-1 and (b) the mutant R9/25/30/54A. The retention times for DAFP-1 and the mutant R9/25/30/54A are 5.00 min and 4.96 min, respectively. The purity of the AFPs was greater than 95%.